

# RELATIONSHIPS BETWEEN FLUID MOTION AND PRESSURE VARIATION BY DAM-BREAK FLOWS COLLIDING WITH VERTICAL WALL

Natsuki Mizutani, Osaka Sangyo University, [mizutani@ce.osaka-sandai.ac.jp](mailto:mizutani@ce.osaka-sandai.ac.jp)  
 Jinji Umeda, Graduate school of Osaka City University, [m17td004@hg.osaka-cu.ac.jp](mailto:m17td004@hg.osaka-cu.ac.jp)

## INTRODUCTION

The 2011 Tohoku Earthquake Tsunami ran up the height of over 40 m and covered over 560 km<sup>2</sup> of the coastal land area in Tohoku, Japan. The tsunami destroyed many structures and killed over 15,000 people. Appropriate measures should be taken against the next giant tsunami to avoid such tragedy. The generation mechanism of wave force is uncertain when a tsunami wave running on land collides with a structure. Especially, the fluid motion of a tip of tsunami wave immediately after the collision with a structure is very complicated. The information of the pressure distribution acting on the structure is necessary to construct buildings in the coastal hazard area. The purpose of this study is to clarify the relationships between the fluid motion and pressure variation by a dam-break flow as a tsunami flow on a dry bed colliding with structures.

## EXPERIMENTAL SETUP

The experimental channel is composed of a head tank, a test section, and a water storage tank. The head tank is a steel box with the length of 1.0 m, the width of 0.39 m and the height of 1.0 m. A gate attached to the head tank opens rapidly by an air compressor to make a dam-break flow representing a tsunami flow on a dry bed. The test section is an open channel made of glass sidewalls and bottom, which is 3.3 m long, 0.39 m wide and 0.3 m high. The acrylic slope of 1/40 gradient (2.0 m long and 0.05 m high) and the flat section connecting to it were installed in the test section so that the Fr number of the dam-break flow could approximate it observed in the field [Hayashi et al., 2013]. The vertical wall, which is 0.39 m wide and 0.3 m high, was set on the flat section at 0.195 m from the end of the slope.

The pressure distributions were measured with 10 kHz by using six pressure transducers located at the center of the wall. All the pressure measurements were synchronized with the high-speed video images acquired with 200 Hz. Furthermore, the vertical velocity fields of the dam-break flow immediately after the collision were captured by using PIV technique. The measurement point illuminated by the laser was located at 0.05m from the near side wall of the channel.

The six cases of reservoir water level (see Table 1) in the head tank were selected by calculating Fr number according to the actual tsunami flows occurred in the past, where  $H$  is the reservoir water level,  $h_{max}$  is the maximum inundation height at the wall,  $V_{max}$  is the maximum velocity at the wall,  $Fr_{max}$  is the maximum Fr number calculated from the time history of the inundation height,  $h$  and the velocity,  $V$ .  $h$  and  $V$  were the values of the passing dam-break flow without the wall.

## EXPERIMENTAL RESULTS

Figure 1 shows the time variation of the non-dimensional pressure and integrated horizontal force synchronized with the PIV images in the case of  $H=9$ cm. The point of zero in X-axis is defined as the beginning of response of ch01. When the tip of the flow reaches the

Table 1 - Experimental conditions

$H$ [cm]	$h_{max}$ [mm]	$V_{max}$ [m/s]	$Fr_{max}$
6	5.49	0.354	2.07
7	7.93	0.540	2.75
8	9.84	0.643	3.24
9	11.78	0.725	3.29
10	14.56	0.784	3.05
11	17.23	0.900	3.99

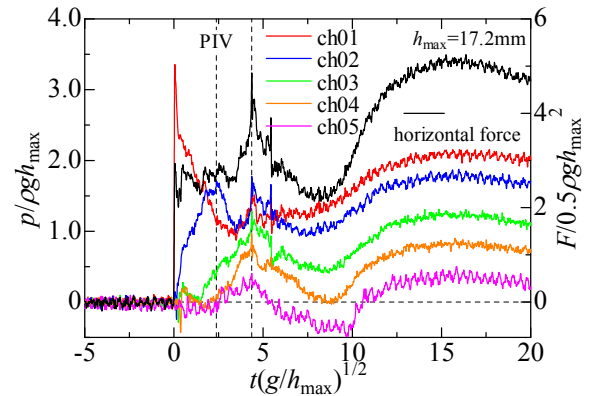


Figure 1 - Time variation of non-dimensional pressure and horizontal force acting on the vertical wall in the case of  $H=9$ cm

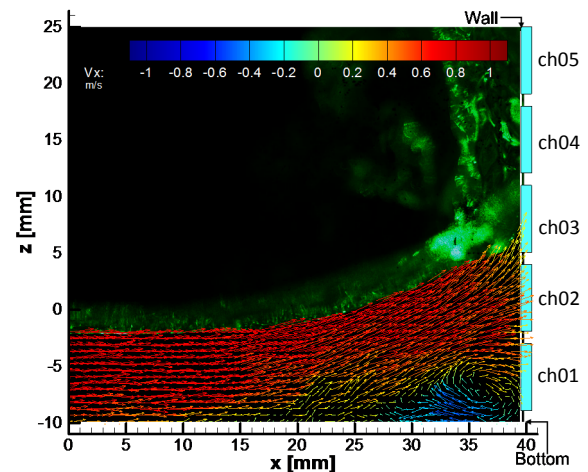


Figure 2 - Internal velocity field in front of the vertical wall at the time of "PIV" indicated in Figure 1

wall, the value of ch01 immediately rises up. The values of the other transducers are nearly equal to zero at that time. As a result, the integrated horizontal force calculated from the values of all the transducers is not large. After that, the value of ch01 drops down and the value of ch02 exceeds that of ch01 after the collision. This behavior of pressure variation can be explained by examining the internal velocity field in front of the wall.

Figure 2 shows the internal velocity field at the time of "PIV" indicated in Figure 1. When the tip of the flow runs up vertically along the wall, the vortex is generated at the

bottom corner of the wall. The following flow avoids the vortex which is almost the same size as a pressure transducer. The flow does not directly hit the transducer of ch01 but ch02 at the upward angle. Therefore, the value of ch02 exceeds that of ch01. The integrated horizontal force is still small at this time.

In Figure 1, the local maximum pressure of each transducer appears at the time of 4.35. These values are generated by the impulsion when the run-up water drops on the following flow (Ramsden et al., 1990). The values of ch01, ch02, and ch03 are very close at this time. Therefore, this pressure distribution does not become the hydrostatic pressure profile and also the integrated horizontal force has the local maximum value. This pressure profile would raise an acting point of the horizontal force higher than the case of the hydrostatic pressure profile. Even when the horizontal force is same, the momentum is larger.

On the other hand, the pressure distribution after the time of about 10 becomes the hydrostatic pressure profile. In this time zone, the water in front of the wall has already stopped moving. The inundation depth in front of the wall dominates the pressure distribution, so the maximum inundation depth is considered as a very important factor for the practical situations. The maximum inundation depth in front of a wall can be estimated as 3 times of the maximum inundation depth of a passing flow without a wall (Asakura et al., 2003). In general, a passing tsunami flow on land can be simulated by using some numerical models. If simulated tsunami flows on land without structures have appropriate values in a numerical model, a horizontal force having a hydrostatic pressure profile can be estimated accurately.

In comparison, the rectangular model (0.08 m long, 0.08 m wide, and 0.2 m high) was used on the flat section instead of the vertical wall.

Figure 3 shows the time variation of non-dimensional pressure in front of the rectangular model in the case of  $H=9$  cm. In the case of the rectangular model, the dam-break flow remains the same, but the maximum impact pressure becomes less than that of the wall. This is because the run-up water spills out from both sides of the model. As a result, the maximum height of the run-up water at the center of the model is lower than that of the wall.

The PIV images were also obtained at the center of the model. The center of the model is about 20 cm far from the side wall of the test section, so the PIV camera can obtain images only in the part lower than the surface level of the following flow.

Figure 4 and Figure 5 show the internal velocity field in front of the rectangular model at the time of "PIV1" and "PIV2" indicated in Figure 3, respectively. In Figure 4, there is the vortex at the bottom corner of the model, which is almost similar to what is shown in Figure 2. In Figure 5, the large-scale circulation is shown in front of the model, because the following flow keeps passing through both sides of the model. Although this circulation is clockwise, there will be another counter-clockwise circulation over the surface level. Therefore, the height of the surface level becomes the divergence point of the flow, so the pressure value at that height will be larger than hydraulic pressure.

## CONCLUSIONS

In this study, the pressure distributions and the internal velocity field were measured by the dam-break

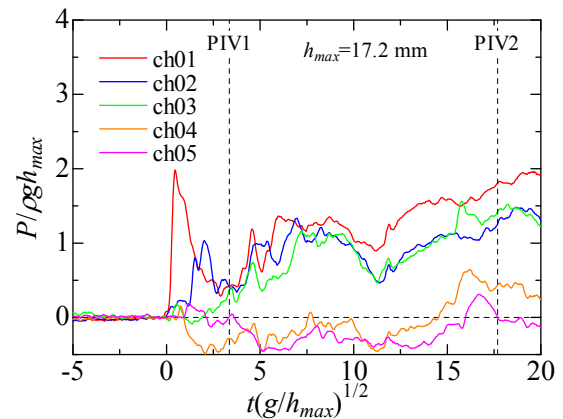


Figure 3 - Time variation of non-dimensional pressure acting on the rectangular model in the case of  $H=9$ cm

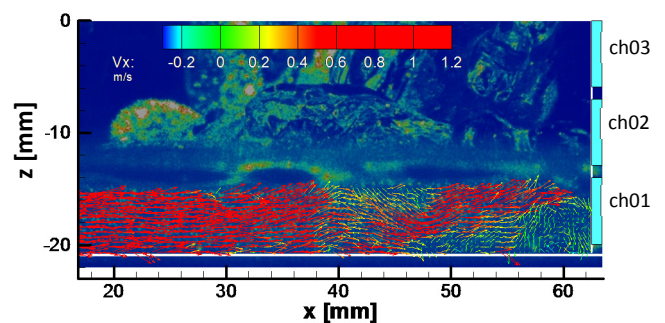


Figure 4 - Internal velocity field in front of the rectangular model at the time of "PIV1" indicated in Figure 3

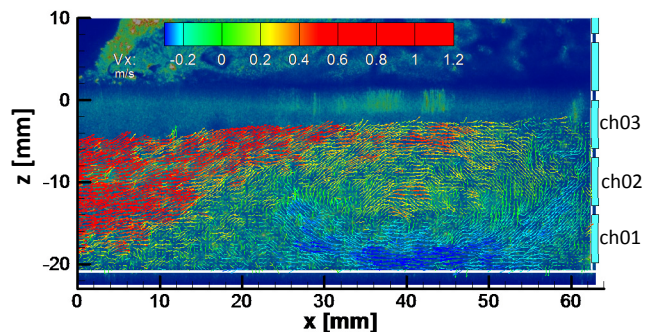


Figure 5 - Internal velocity field in front of the rectangular model at the time of "PIV2" indicated in Figure 3

flow colliding with the vertical wall and the rectangular model. The relationships between the fluid motion and pressure variation immediately after the collision were clarified.

## REFERENCES

- Asakura, R., Iwase, K., Ikeya, T., Takao, M., Fujii, N. and Ohmori, M. (2003): The Tsunami Wave Force Acting on Land Structures, Proc. of 28th ICCE 2002, pp.1191-1202.
- Hayashi, S. & Koshimura, S. (2013): The 2011 Tohoku Tsunami Flow Velocity Estimation by the Aerial Video Analysis and Numerical Modeling, J. Disaster Research, Vol.8(4), pp.561-572.
- Ramsden, J.D. & Raichlen, F. (1990): Forces on Vertical Wall Caused by Incident Bores, J. Waterway, Port, Coastal, and Ocean Eng. Vol. 116(5), pp.592-613.